Optical levitation and translation of a microscopic particle by use of multiple beams generated by vertical-cavity surface-emitting laser array sources

Yusuke Ogura, Nobuhiro Shirai, and Jun Tanida

An optical levitation and translation method for a microscopic particle by use of the resultant force induced by multiple light beams is studied. We show dependence of the radiation pressure force on the illuminating distribution by numerical calculation, and we find that the strongest axial force is obtained by a specific spacing period of illuminating beams. Extending the optical manipulation technique by means of vertical-cavity surface-emitting laser (VCSEL) array sources [Appl. Opt. **40,** 5430 (2001)], we are the first, to our knowledge, to demonstrate levitation of a particle and its translation while levitated by using a VCSEL array. The vertical position of the target particle can be controlled in a range of a few tens of micrometers with an accuracy of 2 μm or less. The analytical and experimental results suggest that use of multiple beams is an effective method to levitate a particle with low total illumination power. Some issues on the manipulation method that uses multiple beams are discussed. © 2002 Optical Society of America

OCIS codes: 140.7010, 250.7260, 140.3290, 120.4640, 350.4990.

1. Introduction

Illumination of a light wave onto an object induces radiation pressure, and the object receives piconewton order of force.[1] Manipulation techniques of the object based on the radiation pressure force are called optical trapping (optical tweezers), and these techniques are applied to a wide variety of fields such as manipulation of biological cells,[2,3] measurement of piconewton force,[4] synthesis of a new macromolecule,[5] and operation of an optical spin micromotor.[6]

Flexible control of the interaction between the illumination light and the target object is essential for optical manipulation of the object, and therefore generation of an appropriate light field is an important issue. Interferometric intensity fields, high-order laser modes, and intrinsic properties of the light such as polarization are effective means to achieve that purpose. An interferometric fringe generated by two or more beams enables us to translate hollow glasses[7] and arrange particles regularly.[8] Using the high-order-mode beam, we can trap low-index particles[9] and rotate a particle.[10] Interaction between the particle and a beam with phase singularity yields momentum transfer, and then the particle rotates.[11] The birefringent particles are aligned or spun depending on the polarization of the light.[12]

Temporal modulation of a single light beam is also an effective way to extend the functionality of the optical manipulation technique. Good examples of temporal modulation methods include arbitrary arrangement of microparticles with fast beam scanning,[13] nonmechanical manipulation of a particle by use of a Fresnel zone plate displayed on a spatial light modulator,[14] and multifunctional manipulation with selective use of computer-generated holograms to control light distribution.[15] The effectiveness of the spatial and temporal modulations of light in the optical manipulation technique is beyond doubt. However, because a single light source is employed, external devices must be used to generate the desired illuminating distribution. In addition, the functionality of the optical manipulation system tends to be restricted by the hardware configuration.

We have presented an optical manipulation method that uses vertical-cavity surface-emitting laser (VCSEL) array sources, called VCSEL array trapping.[16] Because various light distributions can be generated by control of the spatial and temporal

The authors are with Department of Information and Physical Sciences, Graduate School of Information Science and Technology, Osaka University, 2-1 Yamadaoka, Suita, Osaka 565-0871, Japan. The e-mail address of Y. Ogura is ogura@ist.osaka-u.ac.jp.

Received 17 January 2002; revised manuscript received 11 June 2002.

0003-6935/02/275645-10$15.00/0

emissions, VCSEL array trapping is useful for flexible and parallel manipulation of multiple objects with compact hardware and a simple control method. In a previous paper[16] we verified the simultaneous translation of multiple particles and the nonmechanical translation of a particle. However, manipulation was restricted in a two-dimensional plane owing to the low emission power of the individual VCSELs.

To overcome this problem, we attempt to levitate and translate a particle while it is levitated by using the resultant force induced by multiple beams of the VCSEL array sources. Because the total illumination power increases and various illuminating distributions are selected, we can control levitation height and translate the particle while maintaining levitation without mechanical movements. The purpose of this study is twofold: numerical analysis of the radiation pressure force associated with the illuminating distribution and experimental verification of the capability of VCSEL array trapping for levitation and translation of microscopic particles. In Section 2 the resultant force induced by multiple beams is calculated with a ray optics model in order to investigate the dependence of the radiation pressure force on the illuminating distribution. In Section 3 we apply the VCSEL array trapping technique to the levitation of a microscopic particle and its translation while levitated, and the vertical positioning range and accuracy are evaluated. To clarify the features of the method, we measure the minimum power needed to levitate the particle for various illuminating distributions. In Section 4 we discuss features and issues related to manipulation that use multiple beams.

2. Numerical Calculation of Radiation Pressure Force

The calculation method of radiation pressure force by Gauthier and Wallace,[17] which is based on a ray optics model, is extended to obtain the resultant force induced by multiple beams. The calculation model combined with the coordinate system used is shown in Fig. 1. A target particle is a dielectric spherical bead that is illuminated by multiple beams from below. The particle receives gravitational force toward the $-z$ direction. Whenever a light beam reaches the surface of the particle, it reflects and refracts according to the reflection law and Snell's law. The particle is assumed not to absorb the light.

When the momentum of a photon is changed by reflection or refraction, that of the target particle is also changed to preserve the total momentum on the basis of the theorem of conservation of momentum. The momentum change of the single photon is expressed by $\Delta\mathbf{P}$. When the light beam, whose intensity distribution is $I_{\text{inc}}(x, y, z)$, is incident on the particle, the force, $\mathbf{F}$, that the particle receives is expressed by

$$\mathbf{F} = \int \frac{-I_{\text{inc}}}{\Delta E}\,\Delta\mathbf{P}\mathrm{d}S. \tag{1}$$

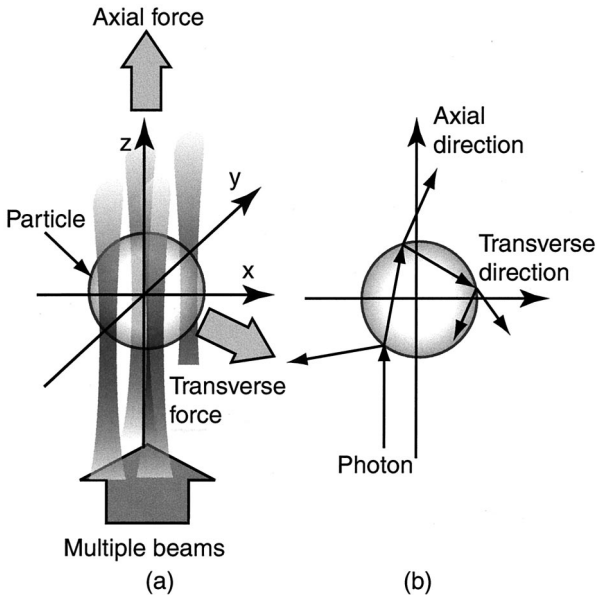

Fig. 1. Model and the coordinate system used for numerical calculation. (a) Incident beams and (b) propagation path of a photon. The dielectric particle is illuminated by multiple beams from below. The calculated radiation pressure force is resolved into axial and transverse forces.

S is the surface of the lower half of the particle, and ΔE is the energy of the single photon expressed by

$$\Delta E = \frac{hc}{\lambda_0}, \tag{2}$$

where h is Planck's constant and λ_0 and c are the wavelength and velocity of the light in vacuum, respectively. $\mathbf{F}$ is resolved into x, y, and z components and expressed as $\mathbf{F} = (F_x, F_y, F_z)$. In this paper $(0, 0, F_z)$ and $(F_x, F_y, 0)$ are called the axial and the transverse forces, respectively.

When the central coordinate of the beam waist is $(X_c, Y_c, 0)$, the intensity distribution of a Gaussian beam is expressed by

$$I_{\text{Gauss}}(x, y, z; X_c, Y_c) = \frac{2P_{\text{Gauss}}}{\pi W_z^{\,2}} \exp\left\{\frac{-2[(x - X_c)^2 + (y - Y_c)^2]}{W_z^{\,2}}\right\}, \tag{3}$$

where

$$W_z = W_0\left(1 + \frac{z^2}{z_0^{\,2}}\right)^{1/2}, \tag{4}$$

$$z_0 = \frac{\pi W_0^{\,2}}{\lambda_0}. \tag{5}$$

P_{Gauss} is the total power of the beam, W_0 is the radius of the beam waist, and z is the axial distance from the beam waist. We assume that illumination $I_{\text{multi}}(x, y, z)$ is composed of N mutually incoherent Gaussian

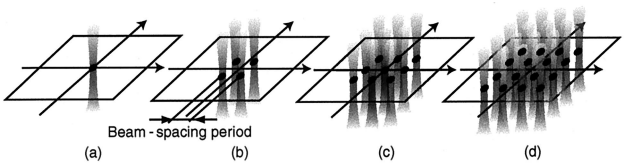

Fig. 2. Illuminating distributions assumed in numerical calculation. (a) 1 beam, (b) 2×2 beams, (c) 3×3 beams, and (d) 4×4 beams. Individual beams focus at $z = 0$.

beams whose central coordinates of the beam waists are $(X_1, Y_1, 0)$, $(X_2, Y_2, 0)$, . . . , $(X_N, Y_N, 0)$; then

$$I_{\text{multi}}(x, y, z) = \sum_{c=1}^{N} I_{\text{Gauss}}(x, y, z; X_c, Y_c). \quad (6)$$

The radiation pressure force is calculated by Eq. (1) with substitution of I_{multi} by I_{inc}.

A set of the illuminating distributions used in the calculation is shown in Fig. 2. The number of the beams associated with the emitting pixels are 1, 2×2, 3×3, and 4×4. The radiation pressure force is calculated with the following parameters: Wavelength λ_0 is 850 nm, the illumination power is 1 mW/pixel, and refraction indices of the particle and the medium (water) are 1.60 and 1.333, respectively. W_0 and the spacing period of the beams are normalized by the radius of the particle r_s and expressed by r_s. The axial position z of the particle is expressed by a parameter α as

$$z = \alpha z_0. \quad (7)$$

In the calculation, we use $W_0 = 0.26 r_s$ and a beam-spacing period of $0.75 r_s$ (the design value for our experimental system).

The relationship between the particle position and the axial force is shown in Fig. 3. This figure displays the force on the plane at $z = 0$, $1.25\, z_0$, $2.50\, z_0$, and $5.00\, z_0$. The strengths of the forces are normalized by the maximum force for individual illuminating distribution and are shown as eight-bit gray-scale images. The maximum axial forces for individual z are summarized in Table 1. The force that the particle in the first quadrant receives is shown in Fig. 3. Owing to the symmetry of the illuminating distribution, the forces in the other quadrants are obtained by rotation of the images in every right angle. The direction of the axial force is usually the $+z$ direction.

As seen from Fig. 3, the axial force changes drastically depending on the particle position for $z = 0$. The position at which the particle receives the maximum force is distant from the origin. However, for $z = 5.00 z_0$, the axial force decreases as the particle moves away from the origin owing to the beam defocus. The particle receives the maximum force at the origin. The maximum force increases with increasing number of beams and decreases for larger z.

Figure 4 shows the dependence of the axial force on z when the particle moves along the z axis. The axial force takes the maximum value at a specific z, which depends on the illuminating distribution, and decreases with increasing z. When $z \leq 2.56 z_0$, the axial force induced by 3×3 beams is stronger than that induced by 4×4 beams at the same z. This shows that an increase in the beam number does not always contribute to the generation of a stronger axial force.

The levitation height is determined as the equilibrium position between the gravitational force and the axial force. The gravitational force F_g is expressed by

$$F_g = \tfrac{4}{3} \pi r_s^3 (\rho_s - \rho_0) g, \quad (8)$$

where ρ_s is the density of the particle, ρ_0 is the density of the medium, r_s is the radius of the particle, and g is the gravitational constant. With the conditions $\rho_s = 1.05$ g/cm^3, $\rho_0 = 1.00$ g/cm^3, and $r_s = 5$ μm, F_g is figured out as 0.256 pN. Table 2 shows the levitation height for different optical powers. For the same total power, the height decreases with an increasing number of beams. When the power of the beam is 1 mW/pixel, a particle 10 μm in diameter cannot be levitated by a single beam but can be levitated by use of multiple beams. This result suggests that we can control the levitation height by switching the illuminating distribution.

Figure 5 shows the dependence of the transverse force on the particle position. This figure is shown in the same fashion as Fig. 3, with arrows to represent the direction of the force. The maximum forces for individual z are summarized in Table 3. We also show, in Fig. 6, the transverse force when the particle moves along (a) the x axis and (b) $y = x$, $z = 0$. Like the axial force, the transverse force intricately varies according to the particle position because the elemental force induced by the individual beams turns in various directions. As a result, the force is not proportional to the number of beams. For the illuminating distribution used in the calculation, the maximum force induced by multiple beams is approximately twice that of a single beam when $z = 0$. The force pushing the target particle outside is obtained by illumination of 4×4 beams for small x and y. For this case, the particle is located at a position distant from the center in the transverse direction.

As seen from Fig. 5, the area in which the particle moves to the origin by the transverse force increases with larger z. However, we cannot avoid a decrease in the transverse force for larger z. The dependence of the maximum transverse force on z when the particle is translated toward the $+x$ direction is shown in Fig. 7. According to Stokes law, translation velocity v can be associated with transverse force F_{trans} and is expressed by

$$F_{\text{trans}} = 6 \pi \eta r_s v, \quad (9)$$

where η is the viscosity of the medium. When a particle with $r_s = 5$ μm is illuminated by 2×2 beams with a spacing period of 3.75 μm, the dependence of the levitation height and maximum transverse velocity toward the $+x$ direction on the total optical power is as shown in Fig. 8. It can be seen that, for exam-

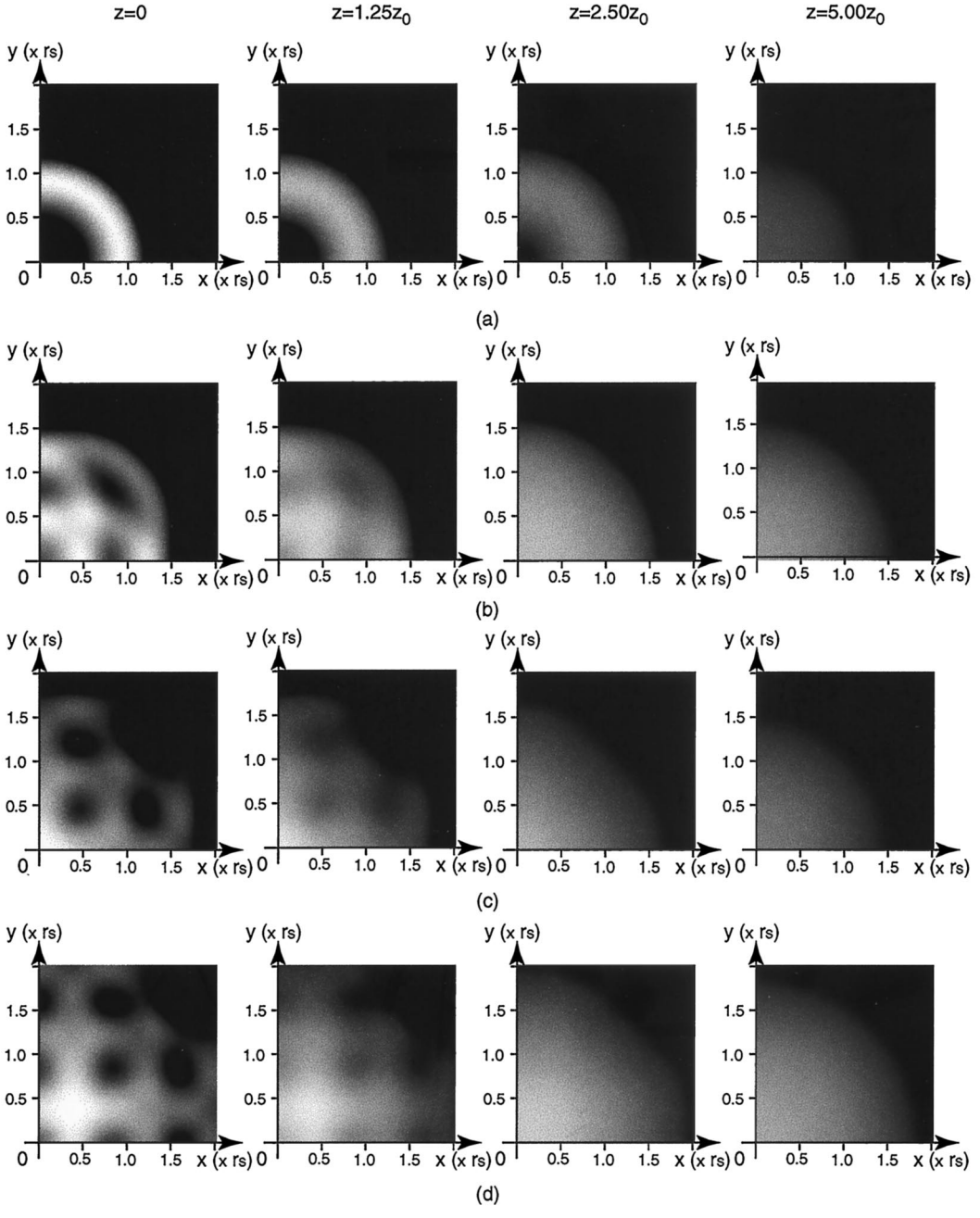

Fig. 3. Relationship between the particle position and the axial force under $W_0 = 0.26r_s$ and beam-spacing period $0.75r_s$. (a) 1 beam, (b) 2×2 beams, (c) 3×3 beams, and (d) 4×4 beams. The particle position (x, y) is normalized by r_s. The maximum forces are (a) 0.688 pN, (b) 1.503 pN, (c) 3.482 pN, and (d) 3.483 pN, by which the the strengths of the forces are normalized and shown as eight-bit gray-scale images.

Table 1. Calculation Results of the Maximum Axial Force on z^a

Number of Beams	Maximum Axial Force (pN)			
	$z(\times z_0)$			
	0	1.25	2.50	5.00
1	0.688	0.493	0.331	0.244
2×2	1.503	1.258	1.093	0.916
3×3	3.482	3.195	2.491	1.749
4×4	3.483	3.219	2.820	2.391

$^a W_0 = 0.26r_s$, and the beam-spacing period is $0.75r_s$.

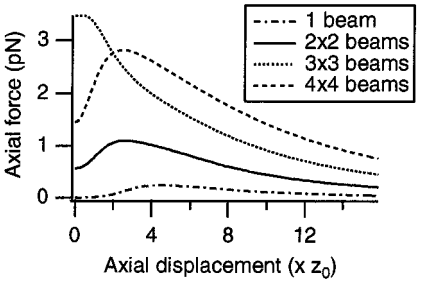

Fig. 4. Dependence of the axial force on z when the particle moves along the z axis. The axial displacement z is normalized by z_0.

Table 2. Calculation Result of the Levitation Height for Different Total Illumination Powers[a]

Number of Beams	Levitation Height (μm)			
	Total Illumination Power (mW)			
	1	2	3	4
1	×	60	77	91
2 × 2	24	57	75	89
3 × 3	18	51	71	86
4 × 4	×	41	64	81

[a]The symbol × indicates that the particle could not be levitated. r_s = 5 μm, W_0 = 1.3 μm, and the beam-spacing period is 3.75 μm.

Table 3. Calculation Result of the Maximum Transverse Force on z[a]

Number of Beams	Maximum Transverse Force (pN)			
	$z(\times z_0)$			
	0	1.25	2.50	5.00
1	1.781	1.387	0.930	0.365
2 × 2	3.323	2.749	2.077	1.062
3 × 3	3.367	2.767	2.430	1.518
4 × 4	3.372	2.766	2.482	1.700

[a]$W_0 = 0.26r_s$, and the beam-spacing period is $0.75r_s$.

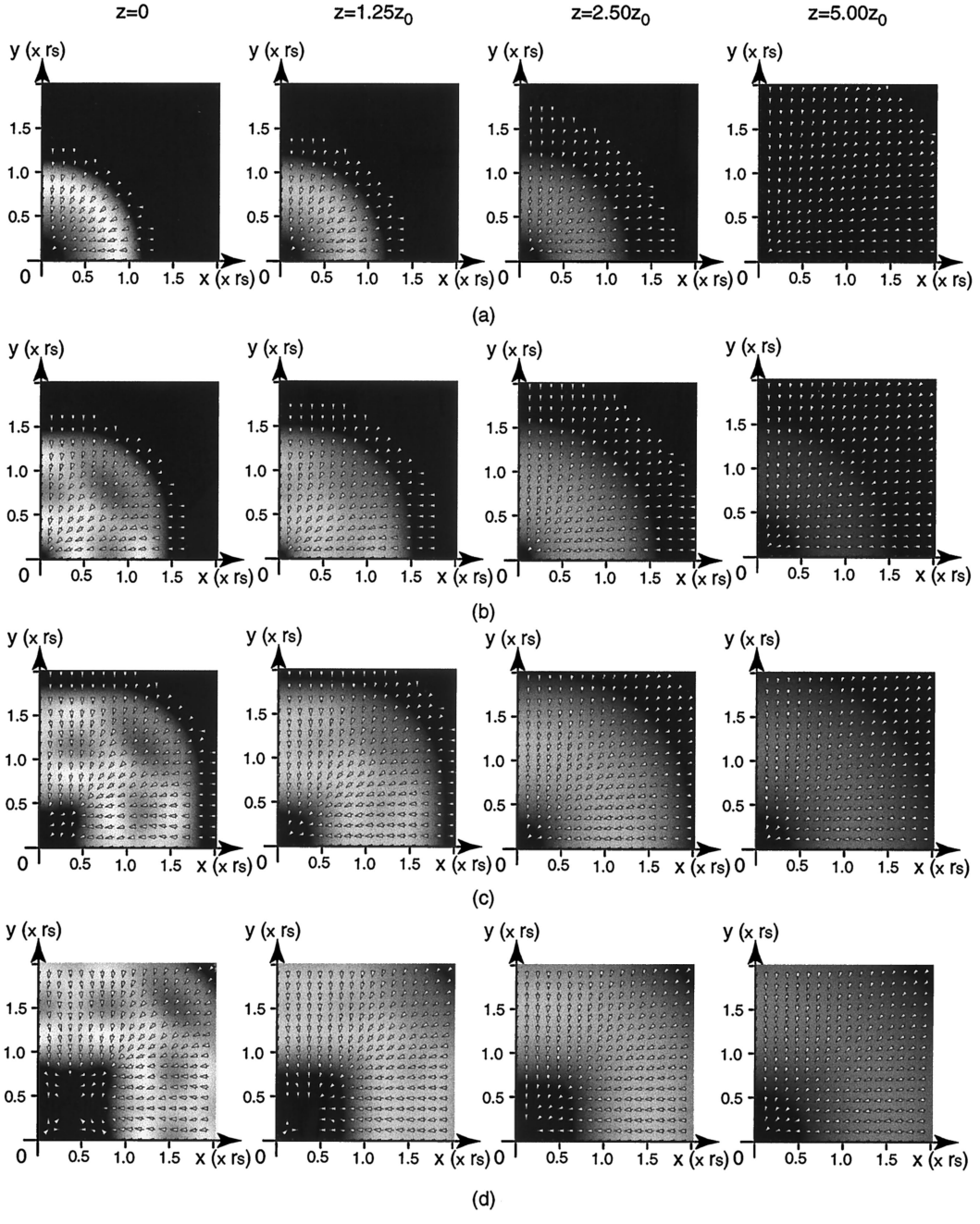

Fig. 5. Relationship between the transverse force and the particle position under $W_0 = 0.26r_s$ and beam-spacing period $0.75r_s$. (a) 1 beam, (b) 2 × 2 beams, (c) 3 × 3 beams, and (d) 4 × 4 beams. The particle position (x, y) is normalized by r_s. The maximum forces are (a) 1.781, (b) 3.323, (c) 3.367, and (d) 3.372 pN, by which the strengths of the forces are normalized and shown as eight-bit gray-scale images.

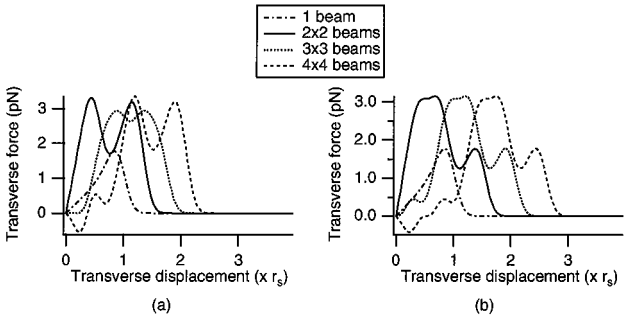

Fig. 6. Dependence of the transverse force on the particle position when the particle moves along (a) the x axis and (b) $y = x$, $z = 0$. The transverse displacement is normalized by r_s.

ple, the velocity at a height of 40 μm is approximately half that at a height of 20 μm. This means that it is more difficult to quickly translate a particle that has a higher levitation. However, if this deceleration is acceptable, we can translate a particle with a levitation height between $z = 20$ μm and 40 μm.

The dependence of the radiation pressure force on the spacing period of the illuminating beams was also investigated. Figure 9 shows (a) the maximum axial force when the particle moves along the z axis and (b) the maximum transverse force when the particle moves along the x axis for individual spacing periods.

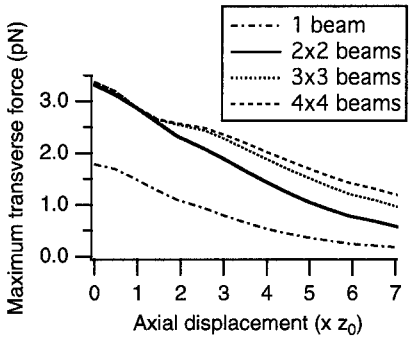

Fig. 7. Dependence of the maximum transverse force on z when the particle moves toward the $+x$ direction. The axial displacement z is normalized by z_0.

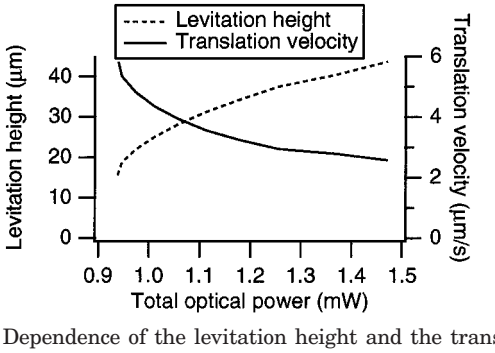

Fig. 8. Dependence of the levitation height and the translation velocity toward the $+x$ direction on the total optical power. The illuminating distribution is 2×2 beams with a spacing period of 3.75 μm and $W_0 = 1.3$ μm. The radius of the particle is 5 μm.

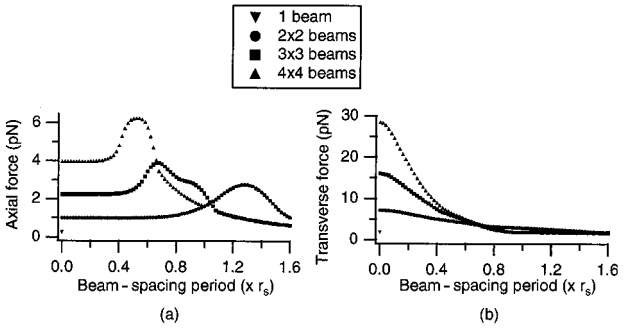

Fig. 9. Dependence of the radiation pressure force on the spacing period of the illuminating beams. (a) Maximum axial force when the particle moves along the z axis and (b) maximum transverse force when the particle moves along the x axis. $W_0 = 0.26r_s$, and the spacing period is varied from 0 to $1.60r_s$ at $0.02r_s$ intervals.

The spacing period is changed from 0 to $1.60r_s$ at $0.02r_s$ intervals.

The transverse force decreases as the spacing period of the beams increases because the forces induced by the individual beams interfere with each other in a wide spacing period. In addition, when the spacing period is in the range of $0.70r_s$ to $1.54r_s$, the transverse force induced by 2×2 beams is

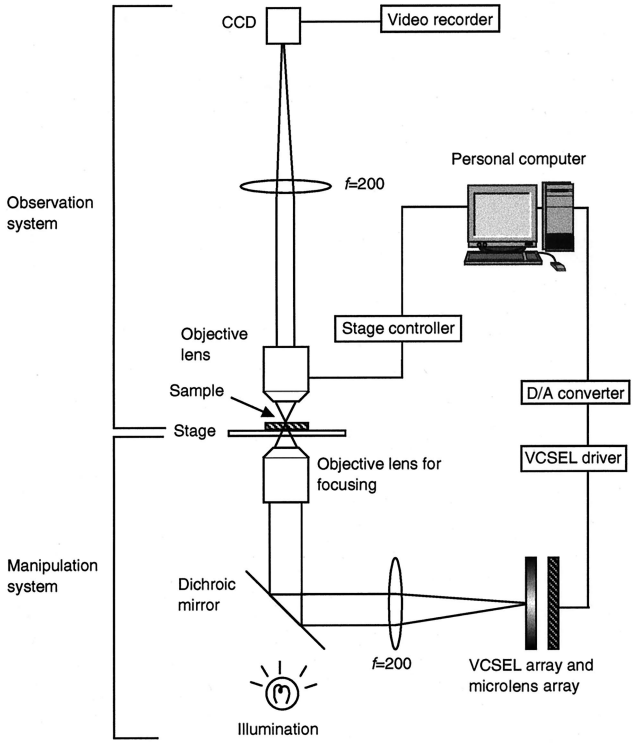

Fig. 10. Experimental setup. 60× (OBJ #1) and 100× (OBJ #2) objective lens are selectively used as the focusing lens of the VCSELs. The lower side of the sample stage is the manipulation system, and the upper side of the sample stage is the observation system. A microlens array is located just behind the VCSEL array to increase light efficiency. The sample chamber can be observed by a CCD and captured by a video recorder. The focusing plane of the observation system is changed when the objective lens of the observation system is moved. D/A, digital to analog.

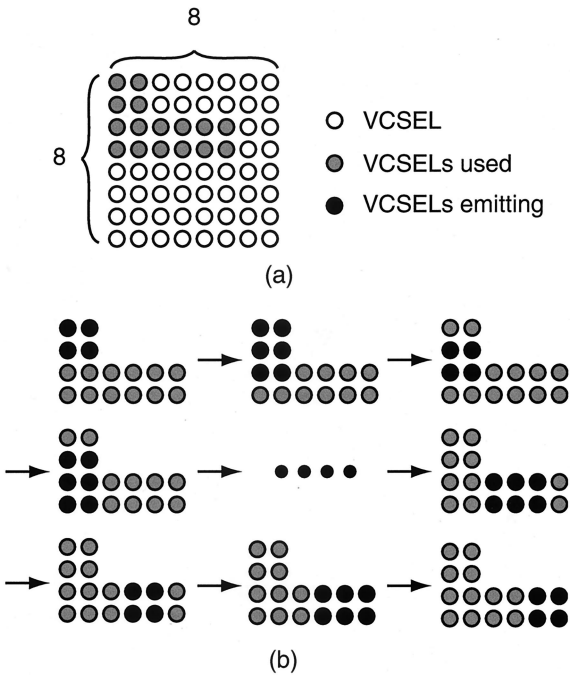

Fig. 11. (a) VCSELs used in the experiment for levitation and translation of the particle and (b) an emission sequence for nonmechanical manipulation. The illuminating distribution is switched manually while the target particle is observed. The averaged illumination power of the 2×2 beams is approximately 3.5 mW.

slightly stronger than that induced by 3×3 beams. In contrast, the axial forces for all the illuminating distributions take the maximum values when the outermost beams of the illumination are located at the boundary of the particle. An explanation for this result is that the momentum transfer of the light incident onto the boundary of the particle is stronger than that onto the center of the particle.[18] This is an interesting feature of optical manipulation that uses multiple beams because it suggests the capability of highly efficient manipulation and flexible control of the object through the appropriate selection of the beam-spacing period. Consequently, the spacing period of the illuminating beams is an important parameter for control of the radiation pressure force.

3. Experimental Results

Figure 10 shows the experimental setup, which is composed of a manipulation system and an observation system. The VCSEL array (NTT Photonics Laboratory; wavelength of 854 nm $\pm$ 5 nm, maximum output of more than 3 mW, aperture of 15 μm in diameter, and pixel period of 250 μm) has 8×8 pixels, whose emission intensities are controlled by driver circuits of our own composition connected to a personal computer. The target object is a polystyrene particle 10 μm in diameter (Polysciences, Inc.; Polybead polystyrene microspheres: refractive index of 1.60 and density of 1.05 g/ml), which is dispersed in water sandwiched between a glass slide and a cover glass. Two water-immersion long-working-distance objective lens [Objective (OBJ) #1: Olympus, LUMPlan Fl 60$\times$ W/IR, and OBJ #2: Olympus, LUMPlan Fl 100$\times$ W) are selectively used for beam focusing. When the VCSEL array pixels are focused on the sample plane, the measured spot radius, the beam-spacing periods, and the intensities at the plane are 1.3 μm, 3.75 μm, and 1.1 mW/pixel for OBJ #1 and 1.1 μm, 2.25 μm and 0.7 mW/pixel for OBJ #2.

We experimentally verified the capability of the VCSEL array trapping technique for optical levitation and nonmechanical translation with levitation. OBJ #1 was used in this experiment. As shown in Fig. 11, 16 pixels in the VCSEL array were used for translation, and these pixels were turned on and off sequentially.

Figure 12 shows the experimental result of the particle levitation and translation. The target particle and its initial position are indicated by a circle and a dot, respectively. During particle manipulation, the objective lens of the observation system was vertically moved to focus on different planes. The procedure for particle manipulation is as follows.

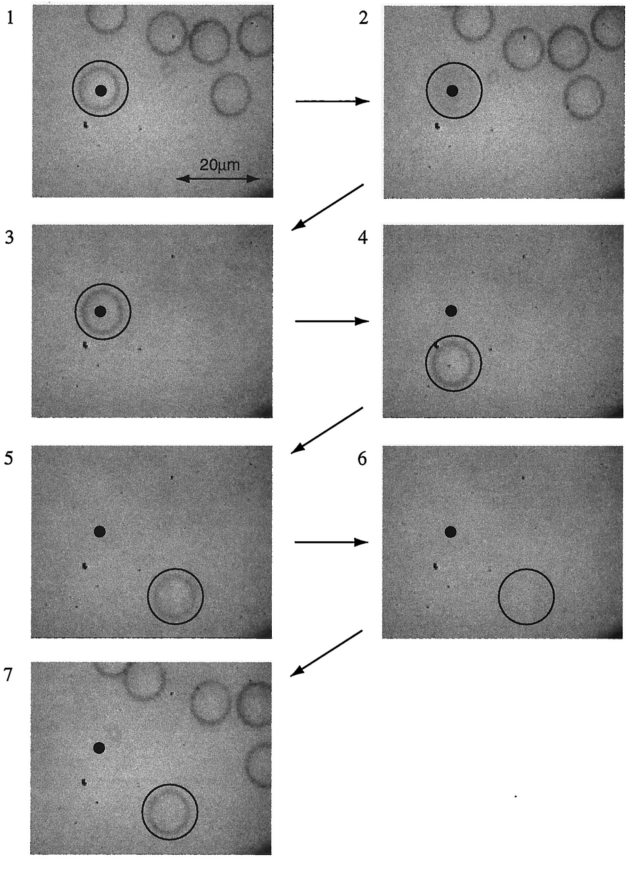

Fig. 12. Experimental result for levitation of the particle and its translation with levitation. The focus of the observation system is moved to observe different planes. The target particle and its initial position are indicated by a circle and a dot, respectively. 1–3: The particle is levitated. 4–5: The particle is translated downward then toward the right. 6–7: The particle falls down on the glass slide.

1. The target particle is captured by 2×2 beams. The observation system focuses on the top surface of the glass slide.
2. The particle is levitated and goes out of focus.
3. The observation system focuses on the target particle. The other particles go out of focus.
4. The particle is translated downward when the emitting pixels are switched.
5. The particle is translated toward the right.
6. All pixels are turned off to release the particle. The target particle goes out of focus because it falls down on the glass slide.
7. The observation system focuses on the top surface of the glass slide.

The pass length of the translated particle is approximately 26 μm, whereas the other particles move up to 10 μm owing to Brownian motion. This experimental result demonstrates that we can (1) levitate the particle and (2) translate the particle while maintaining levitation height by using VCSEL array sources. Note that no mechanical equipment is required for these manipulations.

We can control the vertical position of the particle by moving the beam focus vertically, relative to the sample chamber. We verified this control method by moving the sample stage vertically. Changing the illumination power is another method of controlling the position of the particle. Although the transverse force varies according to the levitation height, it is useful in achieving nonmechanical translation.

To verify this control method, we measured the dependence of the vertical position of the particle on the illuminating power. OBJ #1 was used as the focusing lens. We used the illuminating distributions shown in Fig. 2(b) with a spacing period of 3.75 μm. Figure 13 shows the relationship between the illumination power and the vertical particle position. The error bar is the standard deviation of three measurements. The particle moves higher with stronger illumination power. The positioning range is restricted by the maximum power of illumination. With the experimental system, the particle was translated vertically within a range of a few tens of micrometers by control of the power. The minimum difference between the positions for adjacent sampled illumination power used in the experiment and the standard deviation is 2 μm. From these findings, we concluded that vertical-positioning accuracy in this setup was 2 μm or less.

To illustrate the features of the manipulation method that uses multiple beams, we measured the illumination powers required to levitate the particle for various spacing periods. The optical power required for levitation does not always take the minimum value when the particle is located at the focal plane of the illuminating beams. Therefore we measured the required power under two conditions as follows: (i) We focused the beams at the top surface of the glass slide and increased the power until the target particle is levitated and then measured the power. (ii) We illuminated the particle with a specific power and focused the beams at various planes. If the particle was levitated, the power was measured; if not, we increased the power step by step. The illuminating distribution is shown in Fig. 2(b) for beam-spacing periods of 2.25, 3.75, 4.50, 6.75, and 7.50 μm. OBJ #1 is used for spacing periods of 3.75 and 7.50 μm, and OBJ #2 is used for the spacing periods of 2.25, 4.50, and 6.75 μm.

The relationship between the spacing period of the beams and the power required for levitation is shown in Fig. 14. The curves are the calculation results of the power required to overcome the gravitational force by use of OBJ #1, and the squares and circles show the experimental results. The error bar is the standard deviation of five measurements. Even if the target particle cannot be levitated by condition (i) (the spacing periods of 2.25, 6.75, and 7.50 μm), it can be lifted by use of condition (ii). As seen from Fig. 14, the power depends on the spacing period of the illuminating beams. For a wide spacing period, we can achieve levitation with lower power. This point is predicted by the calculation, though the experi-

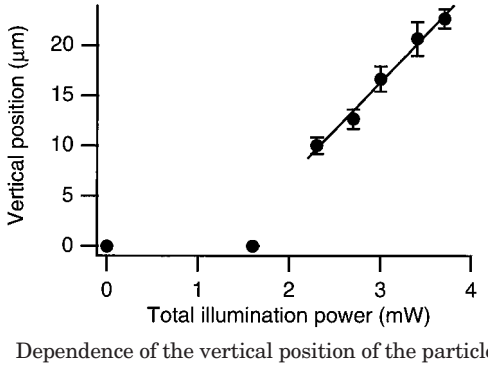

Fig. 13. Dependence of the vertical position of the particle on the total illumination power. The error bar is the standard deviation of three measurements, and the data points are fitted by the line. The illuminating distribution is 2×2 beams with a spacing period of 3.75 μm. The radius of the particle is approximately 5 μm.

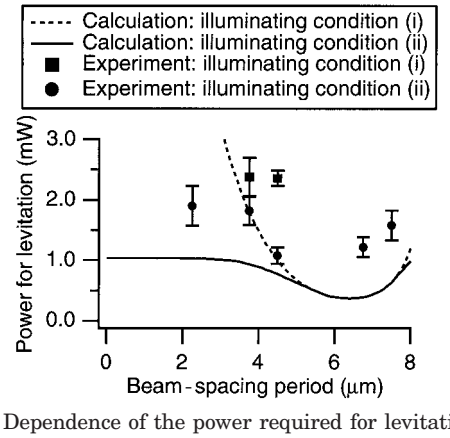

Fig. 14. Dependence of the power required for levitation on the beam-spacing period. Curves, calculation results; squares and circles, experimental results. The illuminating distribution is 2×2 beams. For spacing periods of 2.25, 6.75, and 7.50 μm, the particle could not be levitated under condition (i).

mentally measured power does not exactly agree with the calculation result.

The particle is initially in contact with the surface of the glass slide. Therefore a force stronger than adhesion force and gravitational force is required to levitate the particle from the surface. For example, the adhesion force between a polystyrene particle 0.8 μm in diameter and the glass substrate in a 10-mM potassium nitrate (KNO_3) solution was estimated as 0.2 pN.[19] Because the adhesion force depends on the reaction system, we do not know the exact adhesion force of our system. However, it is thought that the difference between the measured and the calculated power is caused by the adhesion force. Other possible reasons for this difference are the multimode characteristics of the VCSELs and the instability of the particle position in the transverse direction.

4. Discussion

The total illumination power of 4 × 4 beams is 16 times stronger than that of a single beam. From the numerical calculation shown in Fig. 9(a), when the particle is illuminated by 4 × 4 beams with a $0.52r_s$ spacing period, the axial force increases to be approximately 25 times stronger than that of a single beam. This means that, with the same illumination power, we can obtain stronger radiation pressure force by using multiple beams with the appropriate spacing period. This feature is useful for avoiding the damage to a sample, such as a biological cell, caused by strong illumination power.

In the experiment shown in Fig. 14, the particle could not be levitated under condition (i) with spacing periods of 2.25, 6.75, and 7.50 μm. For the 2.25-μm spacing period, shortage of power was the reason, as predicted by numerical calculation. For wide spacing periods of 6.75 and 7.50 μm, a particular beam traps the particle, so that cooperative illumination is not utilized in these cases. By displacement of the focus of the illumination beams along the z direction [condition (ii)], this problem can be avoided; because individual beams spread and overlap when defocused, all the beams function cooperatively.

The calculation and the experimental results clarify that the spacing period of the beams at the sample plane is one of the important parameters for determining the performance of the presented method. Spacing periods suitable for target objects and concrete applications should be selected carefully because the axial and the transverse forces exhibit different behaviors according to the spacing period. The resolution limit of an optical system is typically 1 μm, so the most effective spacing period of the illuminating beams is 0.5 μm according to the sampling theorem. Use of array sources with a small array pitch is a simple solution for achieving this spacing period. An optical system that uses microoptics combined with array sources is also a promising solution. For example, an off-axis type of microlens array is useful for controlling the spacing period because the device provides beam deflection as well as beam focusing with compact configuration.

Using the above spacing period, we can generate a complex light field. However, the translation area is sacrificed because the area is estimated as a product of the beam-spacing period and the pixel number of sources. When the beam-spacing period is 0.5 μm and the number of pixels is 8 × 8, the area in which the particle can be manipulated is limited to 4 μm × 4 μm. Therefore the number of controllable beams as well as the spacing period is important. Fortunately, much effort is being made to increase the pixel number of the VCSEL array. Making use of these techniques and devices, a VCSEL array trapping system capable of manipulating multiple particles with a submicrometer order of accuracy is expected to be developed.

The particle size that can be manipulated is restricted by the beam-spacing period of multiple beams. If the spacing period is wider than the particle size, the forces induced by the individual beams do not work cooperatively, and we cannot capture and translate the object. For the above reason, coupled with the beam-spot size and emission power of the VCSELs, it is thought that the particle size range to which we can apply the presented method is within 1 to 10 μm in diameter. However, it is not impossible to manipulate nanometer-order objects indirectly. In the molecular biology field, for example, the single DNA is knotted, and the tension to be broken is measured by manipulating the beads attached to the DNA.[20] The potential of the VCSEL array trapping for system miniaturization is attractive for microsystem technology such as lab-on-a-chip.[21,22]

5. Conclusion

We have presented analytical and experimental studies on optical levitation and translation of a microscopic object using multiple beams of a VCSEL array. The radiation pressure force on the particle position and the illuminating distribution was shown by numerical calculation. We found that the force strongly depends on the spacing period. It is interesting to note that the strongest axial force is induced by a specific spacing period of illuminating multiple beams. We demonstrated that VCSEL array trapping is capable of levitating the particle and translating it while maintaining levitation height. The vertical position of the particle could be controlled in a range of a few tens of micrometers with an accuracy of 2 μm or less. The required power for levitation by use of multiple beams was experimentally measured, and the result showed the effectiveness of the method in increasing the force with the same illumination power. This is one of the advantages of the manipulation method for microscopic objects that uses simultaneous illumination of multiple beams based on the VCSEL array trapping technique. Owing to its capability of flexible manipulation of multiple objects with compact hardware and a simple control method, VCSEL array trapping should contribute to the exploration of new application fields of optical manipulation.

The VCSEL array was supplied by NTT Photonics Laboratory through the System Photo-Electronics Consortium in Japan. The authors appreciate the support of the consortium for their studies on optoelectronic application systems.

This research was partially supported by the Ministry of Education, Science, Sports, and Culture, Grant-in-Aid for Exploratory Research, 13875015, 2001.

References

1. S. M. Block, "Making light work with optical tweezers," Nature **360,** 493–495 (1992).
2. A. Ashkin and J. M. Dziedzic, "Optical trapping and manipulation of viruses and bacteria," Science **235,** 1517–1520 (1987).
3. A. Ashkin, J. M. Dziedzic, and T. Yamane, "Optical trapping and manipulation of single cells using infrared laser beams," Nature **330,** 769–771 (1987).
4. S. C. Kuo and M. P. Sheetz, "Force of single kinesin molecules measured with optical tweezers," Science **260,** 232–234 (1993).
5. P. Borowicz, J. Hotta, K. Sasaki, and H. Masuhara, "Laser-controlled association of poly(N-vinylcarbazole) in organic solvents; radiation pressure effect of a focused near-infrared laser beam," J. Phys. Chem. B **101,** 5900–5904 (1997).
6. Z. P. Luo, Y. L. Sun, and K. N. An, "An optical spin micromotor," Appl. Phys. Lett. **76,** 1779–1781 (2000).
7. M. P. MacDonald, L. Paterson, W. Sibbett, and K. Dholakia, "Trapping and manipulation of low-index particles in a two-dimensional interferometric optical trap," Opt. Lett. **26,** 863–865 (2001).
8. M. M. Burns, J. M. Fournier, and J. A. Golovchenko, "Optical matter: crystallization and binding in intense optical fields," Science **249,** 749–754 (1990).
9. K. T. Gahagan and G. A. Swartzlander, Jr., "Optical vortex trapping of particles," Opt. Lett. **21,** 827–829 (1996).
10. L. Paterson, M. P. MacDonald, J. Arlt, W. Sibbett, P. E. Bryant, and K. Dholakia, "Controlled rotation of optically trapped microscopic particles," Science **292,** 912–914 (2001).
11. H. He, M. E. J. Friese, N. R. Heckenberg, and H. Rubinsztein-Dunlop, "Direct observation of transfer of angular momentum to absorptive particles from a laser beam with a phase singularity," Phys. Rev. Lett. **75,** 826–829 (1995).
12. M. E. J. Friese, T. A. Nieminen, N. R. Heckenberg, and H. Rubinsztein-Dunlop, "Optical alignment and spinning of laser-trapped microscopic particles," Nature **394,** 348–350 (1998).
13. K. Sasaki, M. Koshioka, H. Misawa, N. Kitamura, and H. Masuhara, "Laser-scanning micromanipulation and spatial patterning of fine particles," Jpn. J. Appl. Phys. **30,** L907–L909 (1991).
14. Y. Hayasaki, M. Itoh, T. Yatagai, and N. Nishida, "Nonmechanical optical manipulation of microparticle using spatial light modulator," Opt. Rev. **6,** 24–27 (1999).
15. J. Liesener, M. Reicherter, T. Haist, and H. J. Tiziani, "Multi-functional optical tweezers using computer-generated holograms," Opt. Commun. **185,** 77–82 (2000).
16. Y. Ogura, K. Kagawa, and J. Tanida, "Optical manipulation of microscopic objects by means of vertical-cavity surface-emitting laser array sources," Appl. Opt. **40,** 5430–5435 (2001).
17. R. C. Gauthier and S. Wallace, "Optical levitation of spheres: analytical development and numerical computations of the force equations," J. Opt. Soc. Am. B **12,** 1680–1686 (1995).
18. N. B. Simpson, D. McGloin, K. Dholakia, L. Allen, and M. J. Padgett, "Optical tweezers with increased axial trapping efficiency," J. Mod. Opt. **12,** 1943–1949 (1998).
19. J. Noordmans, P. J. Wit, H. C. van der Mei, and H. J. Busscher, "Detachment of polystyrene particles from collector surfaces by surface tension forces induced by air-bubble passage through a parallel plate flow chamber," J. Adhes. Sci. Technol. **11,** 957–970 (1997).
20. Y. Arai, R. Yasuda, K. Akashi, Y. Harada, H. Miyata, K. Kinosita Jr., and H. Itoh, "Tying a molecular knot with optical tweezers," Nature **399,** 446–448 (1999).
21. B. H. Weigl and P. Yager, "Microfluidic diffusion-based separation and detection," Science **283,** 346–347 (1999).
22. J. B. Knight, A. Vishwanath, J. P. Brody, and R. H. Austin, "Hydrodynamic focusing on a silicon chip: mixing nanoliters in microseconds," Phys. Rev. Lett. **80,** 3863–3866 (1998).